Quantum Tunneling Currents in a Superconducting Junction

A. H. Worsham,[a] N. G. Ugras, D. Winkler,[b] and D. E. Prober
Department of Applied Physics, Yale University, New Haven, Connecticut 06520-2157

N. R. Erickson and P. F. Goldsmith
Department of Physics and Astronomy, University of Massachusetts, Amherst, Massachusetts 01003
(Received 1 August 1991)

We have measured the full voltage dependence of the quantum conductance and quantum susceptance which arise, respectively, from the dissipative and nondissipative quasiparticle tunneling currents in a superconductor-insulator-superconductor tunnel junction. Using a standing-wave technique, we measured the admittance of the tunnel junction at 87 GHz. The admittance is the sum of the quantum conductance and the quantum susceptance. We report the first direct observation of the reactive quasiparticle singularity which is evident in the quantum susceptance.

PACS numbers: 74.30.Gn, 74.50.+r, 85.25.−j, 84.40.Yw

The currents in a superconducting tunnel junction arise from both pairs and quasiparticles. In the presence of rf radiation, the currents have both dissipative and reactive terms. The pair current has been studied extensively [1,2]. The *dissipative* quasiparticle current determines the dc I-V curve for a voltage biased device. The *reactive* quasiparticle current is observed only in the presence of applied radiation. This current is of interest because of the predicted singularity at the gap voltage which arises in quantum tunneling theory. Also, quasiparticle tunneling is the basis for the most sensitive mixer/receivers up to ≈ 300 GHz. [3]. We shall show that the reactive current might be utilized to provide an *electrically* controlled on-chip tuning element for future THz receivers. In addition, the standing-wave technique which we utilize can be extended to address other issues such as the measurement of the dissipative and reactive currents in a resonant tunneling diode [4].

At high frequencies, $\hbar\omega > e\Delta V$ [3], the response of the tunnel junction must be treated quantum mechanically; ΔV is the voltage width of the current rise at the gap voltage V_g (see Fig. 1). The quasiparticle currents at harmonics of ω and the Josephson currents at the dc voltages used in our experiments are effectively shunted by the junction capacitance, C, and other on-chip admittances [5]. Thus, for an applied voltage $V(t)=V_0+V_\omega\cos\omega t$, with V_0 the dc voltage, the real (in-phase) part of the admittance $Y(V_0,V_\omega)$ is the quantum conductance, given by [3]

$$G_Q(V_0)=\frac{1}{V_\omega}\sum_{n=-\infty}^{\infty}J_n(\alpha)[J_{n+1}(\alpha)+J_{n-1}(\alpha)]I_{\rm dc}(V_0+n\hbar\omega/e) \tag{1a}$$

$$\approx\frac{e}{2\hbar\omega}[I_{\rm dc}(V_0+\hbar\omega/e)-I_{\rm dc}(V_0-\hbar\omega/e)],\ \text{for}\ \alpha\ll 1\,, \tag{1b}$$

where $\alpha=eV_\omega/\hbar\omega$, $I_{\rm dc}(V_0)$ is the dc current at V_0 with $V_\omega=0$, and J_n is the Bessel function of order n. The quantum susceptance is given by $B_Q(V_0)=\mathrm{Im}[Y(V_0,V_\omega)]$; thus [3]

$$B_Q(V_0)=\frac{1}{V_\omega}\sum_{n=-\infty}^{\infty}J_n(\alpha)[J_{n+1}(\alpha)-J_{n-1}(\alpha)]I_{\rm KK}(V_0+n\hbar\omega/e) \tag{2a}$$

$$\approx\frac{e}{2\hbar\omega}[I_{\rm KK}(V_0+\hbar\omega/e)+I_{\rm KK}(V_0-\hbar\omega/e)-2I_{\rm KK}(V_0)]\ \text{for}\ \alpha\ll 1\,, \tag{2b}$$

where $I_{\rm KK}(V_0)$ is the Kramers-Kronig transform of $I_{\rm dc}(V_0)$ and is given by

$$I_{\rm KK}(V_0)=P\int_{-\infty}^{\infty}\frac{dV_0'}{\pi}\frac{I_{\rm dc}(V_0')-V_0'/R_n}{V_0'-V_0}\,, \tag{3}$$

where P is the Cauchy principal value and R_n is the junction normal-state resistance. $I_{\rm KK}(V_0)$ describes the reactive quasiparticle current [1,2,6]. Note that throughout this paper, G_Q, B_Q, C, and all voltages are for an *individual* junction.

Previous work [7] used a resonant technique to determine the quantum conductance and susceptance over a limited bias voltage range ($V_g-2\hbar\omega/e<V_0<V_g$) and for very small input powers ($\alpha\ll 1$), using the junction itself as the detector. That experiment showed agreement with the theoretical predictions for the range studied. The resonant technique is appropriate for a junction with narrow resonance ($\omega R_nC\gg 1$), whereas our technique, described below, is appropriate for a device with broad resonance, as utilized in many practical receivers at mm wavelengths. Further, superconductor-insulator-superconductor (SIS) receivers are usually operated in the regime where $\alpha\approx 1$, where G_Q and B_Q have not been directly measured.

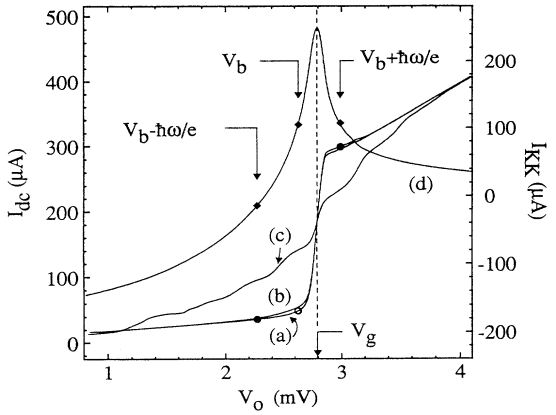

FIG. 1. Current vs dc voltage for a single junction: V_g is the gap voltage. The voltage width of the current rise is $\Delta V = 150$ μV. (a) The measured dc I-V curve with no applied rf signal. The points on the curve are those used in the calculation of G_Q at low power, Eq. (1b), at a particular dc bias voltage, $V_b = 2.625$ mV, indicated by the open circle. The low-power G_Q at V_b is given by the slope of a line (not shown in figure) connecting the two dark circles. (b) The dc I-V curve with low rf power ($\alpha < 0.3$ near V_g) corresponding to G_Q and B_Q of Figs. 3(a) and 3(b). (c) The dc I-V trace with high rf power ($\alpha \geq 1.2$) corresponding to Figs. 3(c) and 3(d). (d) The Kramers-Kronig current calculated from (a). The points on the curve are those used in the calculation of B_Q at low power, Eq. (2b), for $V_b = 2.625$ mV. At V_b, B_Q is negative.

Figure 1 shows the measured dc I-V trace of the device studied [Fig. 1(a)], and its Kramers-Kronig transform [Fig. 1(d)]. The device was a series array of four Nb/AlO_x/Nb junctions, assumed to be identical. The current density was $J_c = 5000$ A/cm^2. The experimental results for a two-junction array were similar to those presented here for the four-junction array. All measurements were performed at 4.4 K. The voltages in Fig. 1 and the rest of the paper are scaled to show the voltage per junction in order to relate the experimental results to the theoretical predictions for a single junction [8]. For low input rf powers, $\alpha \ll 1$, only single-photon processes are allowed. (In a series array, the single photon process corresponds to each junction absorbing or emitting a single photon.) For $\alpha \ll 1$, G_Q is simply a first finite difference, given by Eq. (1b). B_Q of Eq. (2b) is a second finite difference. At voltage V_g there is a singularity in B_Q due to the singularity in the Kramers-Kronig current at V_g [Fig. 1(d)]. This singularity has not been directly observed prior to this work.

The equivalent circuit used in the analysis and a schematic of the standing wave are shown in Fig. 2. In order to measure the junction array admittance over the entire range of dc voltage and input power, we used a waveguide slotted-line technique [9]. A 29-GHz signal was tripled to generate the 87.1-GHz radiation. This was coupled at 4.4 K from the waveguide into the device through a Chebychev ridge transformer and quarter-

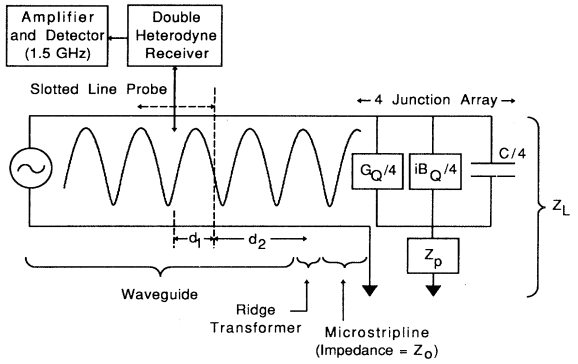

FIG. 2. The equivalent circuit used in the analysis and a schematic of the experimental apparatus. The voltage standing wave is shown schematically. G_Q, B_Q, and C are for a single junction. The ridge transformation is essentially perfect. The microstripline is one-quarter wavelength long.

wavelength microstripline [5]. The coupling scheme was originally designed for work with SIS mixers and achieves a simple broadband transformation of the high-impedance waveguide to the 50-Ω microstripline feeding the junction array. The properties of our coupling structure are well studied; reflections from the ridge are minimal [10]. Any impedance mismatch between the tunnel junction array and the microstripline caused a standing wave to form along the microstripline and the waveguide. The amplitude and phase of the standing-wave pattern were measured with a weakly coupled probe inserted into a slotted line in the waveguide at room temperature. The 87.1-GHz radiation coupled into the probe was heterodyned twice down to 1.5 GHz [11]. This 1.5-GHz signal was amplified and then detected with a diode power detector. Analysis of the standing wave allowed determination of G_Q and B_Q. We used an array of tunnel junctions to allow larger input powers for a given α, to obtain a better signal-to-noise ratio for the measurement.

A standing wave formed due to the mismatch between the characteristic impedance of the microstripline, $Z_0 \approx 50$ Ω in this work, and the terminating impedance, Z_L. From Fig. 2, $Z_L = Z_p + 4[i\omega C + G_Q + iB_Q]^{-1}$; the factor of 4 is due to having a four-junction array. Z_p is due to the passive on-chip terminating circuitry after the tunnel junctions, primarily a quarter-wavelength radial stub. Z_p is determined from scale model results [10] to be $-i5$ Ω at 87.1 GHz. Using published values of the specific capacitance of Nb/AlO_x/Nb tunnel junctions [12] of 45 ± 5 fF/(μm)^2 and the lithographic area, a value of $\omega C = 98.8$ mmhos was used in the analysis. The mismatch equation is $\rho e^{i\theta} = (Z_L - Z_0)/(Z_L + Z_0)$, with ρ the amplitude and θ the phase of the reflection. Other system reflections were negligible. Note that the only dependence of Z_L on V_0 is through the quantum effects of the tunnel junction array itself.

The measured standing-wave power was normalized

to the incident power, determined by terminating the waveguide with a matched load close to the slotted line probe. The normalized standing-wave power is [13]

$$\frac{P}{P_{\text{inc}}} = |[1+\kappa\rho e^{i[\theta-4\pi(d_1+d_2)/\lambda-\pi]}]|^2$$
$$= 1+(\kappa\rho)^2+2\kappa\rho\cos[\theta-4\pi(d_1+d_2)/\lambda-\pi], \quad (4)$$

where $\kappa\rho$ is the amplitude of the reflected wave ($0\leq\kappa\rho\leq 1$), $d=d_1+d_2$ is the distance between the probe and the microstripline (shown in Fig. 2), $[\theta-4\pi(d_1+d_2)/\lambda-\pi]$ is the phase of the reflected wave with the factor of π due to the quarter-wave microstripline, $\lambda=4.70$ mm is the wavelength in the waveguide, and $\kappa=\kappa(d)$ is the round-trip attenuation factor. Over the 3-mm length along the waveguide for which the probe was moved, $\kappa(d)\approx\text{const}\approx 0.3$. Each data set was taken at a fixed value of d_1, with V_0 varied incrementally. The experiment determined $\kappa\rho$ and $(\theta-4\pi d_2/\lambda)$ by least-squares fitting the measured data for various d_1 at a fixed value of V_0, using Eq. (4). The quantities $4\pi d_2/\lambda$ and κ were determined from measurements at a voltage well above the gap voltage. Here, $G_Q=R_n^{-1}$ and $B_Q=0$, so ρ and θ can be computed reliably for $V_0\gg V_g$. $G_Q(V_0)$ and $B_Q(V_0)$ at other values of V_0 were then inferred from the measured values of $\kappa\rho$ and $(\theta-4\pi d_2/\lambda)$ using the mismatch equation and the expression for Z_L given previously.

A comparison of the predicted and experimentally determined G_Q and B_Q is shown in Fig. 3. As in Fig. 1, G_Q and B_Q are for a single junction. The theoretical curves were generated using Eqs. (1a) and (2a) and the equivalent circuit of Fig. 2. In Fig. 3(a), G_Q is for low powers ($\alpha<0.3$ near V_g), and shows reasonably good agreement with the theoretical predictions. G_Q is clearly large and fairly constant for V_0 within one photon width ($\pm\hbar\omega/e$) of the gap voltage, as expected. (Note: $2\hbar\omega/e=720$ μV.) The experimentally inferred magnitude of G_Q within one photon width of the gap was affected by the choice of circuit parameter values in the equivalent circuit. Since B_Q partially resonated the capacitance of the junction array near the gap voltage, much of the measured reflection near the gap voltage was due to the mismatch between Z_0 and $Z_L\approx[(4/G_Q)+Z_p]$. The peak seen in the inferred experimental value of G_Q at the gap voltage was reduced if we used a value of $Z_0=55$ Ω in the equivalent circuit; this is shown by the dashed line in Fig. 3(a). Taking $Z_0=55$ Ω had a negligible effect on the deduced value of B_Q. Since we have not been able to independently confirm the precise value of Z_0 in the experimental apparatus, we used the design value of $Z_0=50$ Ω in our analysis. From the scale modeling, the expected range in Z_0 is 42–60 Ω [10].

The low-power data for B_Q [Fig. 3(b)] shows the singularity at the gap voltage corresponding to the singularity in the reactive quasiparticle current. The experimentally inferred G_Q and B_Q for high input powers

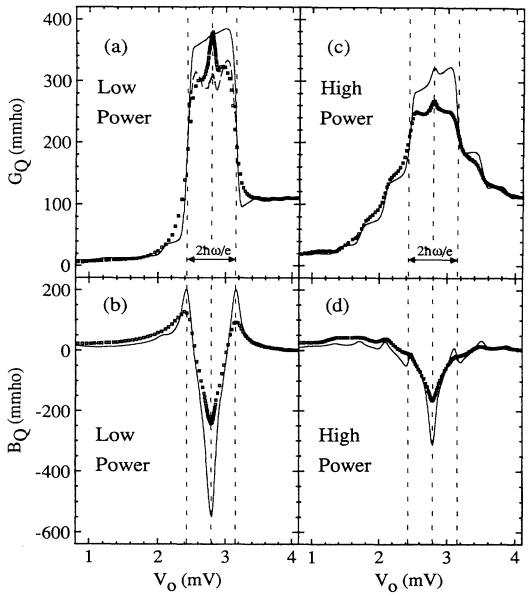

FIG. 3 Values of G_Q and B_Q vs dc voltage for an individual junction deduced from the experiment using $Z_0=50$ Ω; squares are the experimental data and the solid curves are the theoretical predictions. The dashed vertical lines show the bias voltages corresponding to (from left to right) one photon width below the gap, $V_g-\hbar\omega/e$, the gap voltage, V_g, and one photon width above the gap, $V_g+\hbar\omega/e$. (a) G_Q at low power ($\alpha<0.3$ near V_g). The deduced G_Q for $Z_0=55$ Ω is also shown as the dashed line. (b) B_Q at low power. (c) G_Q at high power ($\alpha\geq 1.2$). (d) B_Q at high power.

($\alpha\geq 1.2$) are shown in Figs. 3(c) and 3(d). These show features associated with multiphoton processes, as expected. The lack of "sharpness" in the experimental data may be due to frequency instability in the rf generator ($\sim$10 MHz), since data were taken at fixed values of d_1, not at fixed V_0. Additional rounding may be due to noise in the rf generator or nonuniform junction properties. The shape of the dc I-V curves in the presence of the rf radiation gave evidence that the junctions in the array were not identical. These I-V curves could not be fitted completely consistently with theoretical predictions, whereas similar I-V curves for a single junction were better fitted by the theory. The proximity effect due to the unoxidized Al and the uncertainties in the equivalent circuit parameters may also influence the deduced values of G_Q and B_Q.

There are a number of applications of this work for future THz receivers. The voltage dependence of B_Q could be exploited as an electrically tuned inductor. One would use an array of SIS tunnel junctions which is dc biased independent of, but in rf parallel with, a mixer SIS junction. The array would provide the variable inductance which might be needed to fine tune, over a broad frequency range, the resonant rf coupling to the mixer junction. Also, such an electrically tuned inductor could compen-

sate for some variation of capacitance due to lithographic variations. The dc voltage dependence of G_Q might also be used as a variable attenuator for the local oscillator, if separately coupled to the mixer.

In summary, we have made the first direct measurement of the full dependence on bias voltage of the quantum conductance and quantum susceptance in an SIS tunnel junction. Our results show clearly the singularity in the quantum susceptance at the gap voltage. The results show reasonably good agreement with theoretical predictions both for small and large input powers and verify the existence of the reactive quasiparticle currents, an important prediction of the tunneling Hamiltonian model [14]. The measurement technique we used could also be employed to measure the admittance of a resonant tunneling diode [4]. Since the quantum tunneling theory [14] treats just elastic tunneling, the technique might be used to separate rf currents which arise due to coherent (elastic) resonant tunneling from those which arise due to noncoherent, sequential processes [15].

This work was supported by the NSF Grants No. ECS 8604350, No. AST 88-15406, No. AFOSR-88-0270, and the Swedish National Board for Technical Development. We wish to acknowledge assistance in fabrication from J. H. Kang and J. X. Przybysz at the Westinghouse Science and Technology Center and M. J. Rooks at the National Nanofabrication Facility.

---

[a]Present address: Department of Physics, State University of New York, Stony Brook, NY 11794-3800.

[b]Present address: Department of Physics, Chalmers University of Technology, S-41296, Gothenburg, Sweden.

[1] B. D. Josephson, Phys. Lett. **1**, 251 (1962).

[2] N. R. Werthamer, Phys. Rev. **147**, 255 (1966).

[3] J. R. Tucker and M. J. Feldman, Rev. Mod. Phys. **57**, 1055 (1985); the requirement that $\hbar\omega > e\Delta V$ is the same as that for seeing strong quantum effects with SIS heterodyne mixers.

[4] H. C. Liu, Phys. Rev. B **43**, 12538 (1991).

[5] D. Winkler, N. G. Ugras, A. H. Worsham, D. E. Prober, N. R. Erickson, and P. F. Goldsmith, IEEE Trans. Magn. **27**, 2634 (1991).

[6] R. E. Harris, Phys. Rev. B **11**, 3329 (1975).

[7] Qing Hu, C. A. Mears, P. L. Richards, and F. L. Lloyd, Phys. Rev. Lett. **64**, 2945 (1990).

[8] S. Rudner, M. J. Feldman, E. Kollberg, and T. Claeson, IEEE Trans. Magn. **17**, 690 (1981).

[9] P. A. Matthews and I. M. Stephenson, *Microwave Components* (Chapman and Hall, London, 1968), Chap. 11.

[10] D. Winkler, N. G. Ugras, A. H. Worsham, D. E. Prober, N. R. Erickson, and P. F. Goldsmith, in *Proceedings of the Fifteenth International Conference on Infrared and Millimeter Waves, Orlando, Florida, 1990* (International Society for Optical Engineering, Bellingham, WA, 1990), p. 265.

[11] The 87.1-GHz free-running tripled yttrium iron garnet oscillator signal was mixed down to 7.5 GHz in a balanced Schottky receiver with extremely low local-oscillator leakage using a Gunn-effect local oscillator at 79.6 GHz. No effects of the 79.6-GHz signal were found in the standing wave. An isolator was used to isolate the 87.1-GHz signal from harmonics of the 79.6-GHz signal. The 7.5-GHz signal was amplified and then mixed down to 1.5 GHz in a diode mixer.

[12] A. W. Lichtenberger, C. P. McClay, R. J. Mattauch, M. J. Feldman, S.-K. Pan, and A. R. Kerr, IEEE Trans. Mag. **25**, 1247 (1989); S. Han, J. LaPointe, and J. E. Lukens, Phys. Rev. Lett. **63**, 1712 (1989).

[13] R. L. Liboff and G. C. Dalman, *Transmission Lines, Waveguides, and Smith Charts* (Macmillan, New York, 1985), Chap. 4.

[14] M. H. Cohen, L. M. Falicov, and J. C. Phillips, Phys. Rev. Lett. **8**, 316 (1962).

[15] K. K. Choi, B. F. Levine, C. G. Bethea, J. Walker, and R. J. Malik, Phys. Rev. Lett. **59**, 2459 (1987); M. Büttiker, IBM J. Res. Develop. **32**, 63 (1988).